PAPER

Hall conductance in graphene with point defects

IOP PUBLISHING JOURNAL OF PHYSICS: CONDENSED MATTER

J. Phys.: Condens. Matter **25** (2013) 055302 (10pp) doi:10.1088/0953-8984/25/5/055302

Hall conductance in graphene with point defects

S İslamoğlu, M Ö Oktel and O Gülseren

Department of Physics, Bilkent University, 06800 Ankara, Turkey

E-mail: selcen@fen.bilkent.edu.tr, oktel@fen.bilkent.edu.tr and gulseren@fen.bilkent.edu.tr

Received 31 August 2012, in final form 19 December 2012
Published 8 January 2013
Online at stacks.iop.org/JPhysCM/25/055302

Abstract

We investigate the Hall conductance of graphene with point defects within the Kubo formalism, which allows us to calculate the Hall conductance without constraining the Fermi energy to lie in a gap. For pure graphene, which we model using a tight-binding Hamiltonian, we recover both the usual and the anomalous integer quantum Hall effects depending on the proximity to the Dirac points. We investigate the effect of point defects on Hall conduction by considering a dilute but regular array of point defects incorporated into the graphene lattice. We extend our calculations to include next nearest neighbor hopping, which breaks the bipartite symmetry of the lattice. We find that impurity atoms which are weakly coupled to the rest of the lattice result in gradual disappearance of the high conductance value plateaus. For such impurities, especially for vacancies which are decoupled from the lattice, strong modification of the Hall conductance occurs near the $E = 0$ eV line, as impurity states are highly localized. In contrast, if the impurities are strongly coupled, they create additional Hall conductance plateaus at the extremum values of the spectrum, signifying separate impurity bands. Hall conductance values within the original spectrum are not strongly modified.

(Some figures may appear in colour only in the online journal)

1. Introduction

External magnetic field is a powerful tool to manipulate and tune the properties of condensed matter systems. For example, in applying magnetic field to two-dimensional (2D) electron systems amazing properties such as the Hall effect or the Landau level spectrum emerge. The effect of perpendicular magnetic field on 2D Bloch electrons has been a very active research field since the discovery of the Hofstadter butterfly [1] for the square lattice. It has become a well studied problem since then, and this self-similar structure of energy spectrum is established for various types of 2D lattice [2–9]. These unusual energy spectra gave rise to new questions such as how the conductance and transport properties evolve under magnetic field. In general, 2D systems experiencing a perpendicular magnetic field display the Hall effect. In 1982, it was reported that the Hall conductance for a square lattice is quantized with e^2/h, and it is value is equal to Thouless–Kohmoto–Nightingale–den Nijs (TKNN) integers multiplied by the conductance quantum when the Fermi level lies in energy gaps [10, 11]. Within a gap, the Hall conductance is constant, forming a conductance plateau. These TKNN integers are given by topological invariants known as Chern numbers. For the square lattice these Chern numbers satisfy a Diophantine equation, which can be used to determine conductance in a gap uniquely. However, for other lattices a Diophantine equation does not uniquely determine the conductance. In general, conductance can be calculated by the Streda [12] formula originating from the linear response theory, or by the Kubo formalism.

Graphene, after isolation as a single layer by mechanical exfoliation [13, 14], is one of the most studied systems in recent years. Graphene exhibits several unusual properties because of the Dirac points constituting its band structure. For example, the unconventional quantum Hall effect was predicted in earlier calculations [15, 16]. Soon after the discovery of the anomalous integer quantum Hall effect in graphene [17, 18], many theoretical studies discussing Hall conductance in the low magnetic field regime were reported [5, 19–22]. Hasegewa and Kohmoto calculated the Hall conductance for the plateaus from the Streda formula [5]. They found the Hall conductances are given by $\sigma_{xy} =$

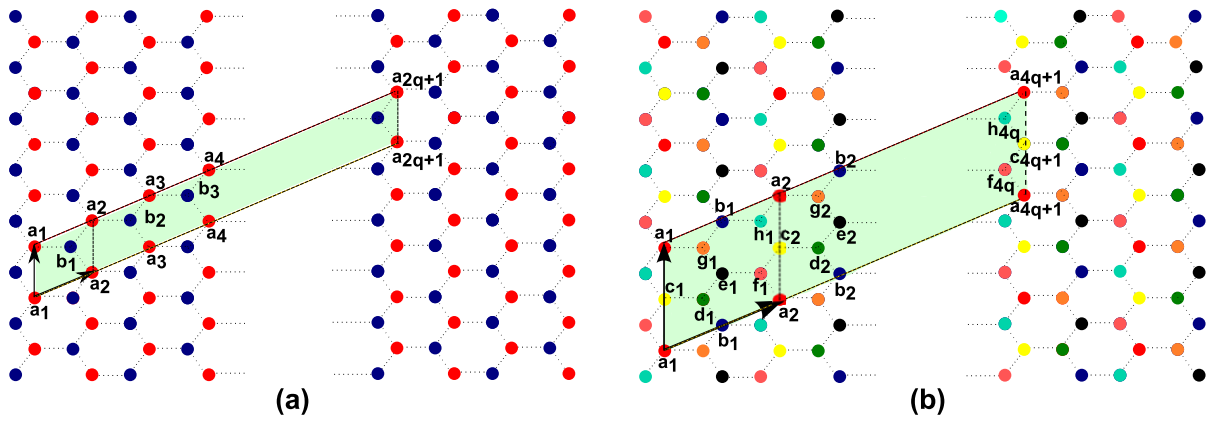

Figure 1. (a) Magnetic unit cell of graphene, in which $4q$ atoms are connected. The unit cell with a basis of two atoms is indicated within the smaller parallelogram. (b) Larger magnetic unit cell of graphene suitable for point defect calculations through which $32q$ atoms are connected. The unit cell has eight atoms in the basis shown within the boundaries of the smaller parallelogram, and the atom labeled '**e**' is the defect atom.

$2ne^2/h$ with $n = \ldots, 3, 2, 1, 0$, in the high magnetic field regime, where the additional factor of 2 arises from the spin degeneracy. In this paper, we follow the tight-binding approximation for the honeycomb lattice in the presence of magnetic field. After diagonalization of the Hamiltonian, we use the corresponding eigenvalues and the eigenvectors in the Kubo formula to calculate the Hall conductance. We come up with $\sigma_{xy} = 2ne^2/h$ with $n = \ldots, 3, 2, 1, 0$ for the high magnetic field limit. Similarly, in the lower magnetic field regime, we observe the anomalous integer quantum Hall effect given by $\sigma_{xy} = 2(2n+1) \times e^2/h$ with $n = \cdots, 3, 2, 1, 0$. Our results for pure graphene are in accordance with experiments and previous calculations.

However, no real sample is defect free. Even in the cleanest material there are point defects such as impurities or vacancies. These defects might be introduced intentionally in order to improve some materials property [23–29]. Therefore, it is essential to understand the effect of these defects on properties such as magnetoconductance [30]. Here, we investigate in detail the evolution of conductance with respect to presence of point defects such as vacancy and impurity atoms in graphene. The effect of uniform on-site disorder on the graphene quantum Hall effect was investigated on a graphene ribbon [31]. A disorder model more relevant to graphene can be constructed by explicitly introducing impurities with modified hopping strength in a supercell approach. In this paper, we present such a model, in which we obtain a 12.5% concentration by treating one atom as a point defect out of eight atoms in the enlarged unit cell. By altering the hopping constant(s) of this impurity atom we model different impurity atoms in graphene, and by setting the hopping constant(s) to zero we model the vacancy case. We show that the impurity atoms with smaller hopping constant than the rest of the atoms result in highly localized states, which do not provide any contribution to the Hall conductance. However, the impurity atoms with higher hopping constant produce delocalized states, which form their own bands [32]. Previously, we have obtained the energy spectrum in the presence of point defects and transverse magnetic field by using the tight-binding method [32]; in this study we investigated the topological nature of that spectrum by evaluating the Hall conductance using the Kubo formula.

The paper is organized as follows: in section 2.1, we summarize the Kubo formalism for the calculation of the Hall conductance for pure graphene. We model graphene with point defects in section 2.2. We discuss the Hall conductances for perfect and imperfect graphene in section 3, then we briefly conclude in section 4.

2. Methodology

2.1. Pure graphene

Graphene has a honeycomb lattice structure with two atoms in its unit cell. The bond distance is 1.42 Å, and each atom has three nearest neighbors. We considered the isotropic case, in which the hopping parameter for the p_z orbitals interacting with the nearest neighbors is equal to -2.66, and -0.1 eV for the next nearest neighbors [33].

When the well known tight-binding method is applied with the Peierls substitution [34] for the Landau gauge $\vec{A} = (0, Bx, 0)$, we end up with Harper's equation [35]. By applying the Bloch condition, Harper's equation is written as an eigenvalue equation, where the $4q \times 4q$ A_m matrix is the Hamiltonian. The elements of this matrix are composed of the interactions over the entire magnetic unit cell, shown in figure 1(a).

The amount of flux per unit cell is given by $\phi = \frac{p}{q}\phi_0$, where the flux quantum $\phi_0 = h/e$. We consider the cases for which p and q are mutually prime integers. The system has a new unit cell under the magnetic field, which is called the magnetic unit cell. In this unit cell, due to the magnetic periodicity and the basis, now $4q$ atoms are connected, as shown in figure 1(a). We have new lattice vectors for this case, which have lengths depending on the parameter q. As we increase q, our magnetic unit cell is enlarged as opposed to the magnetic Brillouin zone. Increasing q has another consequence, such that it yields lower magnitude

for the magnetic field. Since we have to solve eigenvalue equations among the whole Brillouin zone, increasing q brings computational cost for the diagonalization; however, our magnetic Brillouin zone scales down with q, requiring summation over fewer k points. The eigenvalues of the A_{m} matrix are the energy eigenvalues, which yield the Hofstadter butterflies for graphene as a function of flux $\alpha = p/q$ [1, 6]. The detailed description of the tight-binding method applied to pure and defective graphene under magnetic field has been published previously in [32].

Once the eigenvalues and corresponding eigenstates are obtained, the Hall conductance can be calculated from the Kubo formula [10]:

$$\sigma_{xy} = \frac{\mathrm{i}e^2}{A_0\hbar} \sum_{E_\alpha<E_f} \sum_{E_\beta>E_f} [(\partial\hat{H}/\partial k_1)_{\alpha\beta}(\partial\hat{H}/\partial k_2)_{\beta\alpha} - (\partial\hat{H}/\partial k_2)_{\alpha\beta}(\partial\hat{H}/\partial k_1)_{\beta\alpha}][(E_\alpha - E_\beta)^2]^{-1}. \quad (1)$$

The derivative expressions are the velocity matrix elements. The sums over energies above and below the Fermi energy also imply a summation over the magnetic Brillouin zone. The energy eigenvalues are grouped into occupied (α) and unoccupied (β) states. So, by changing the Fermi energy we can calculate the Hall conductance for a given system. This sweep of Fermi energy corresponds to the change in the gate voltage in the usual quantum Hall experiments. Similar calculations based on this approach have been carried out for other lattice geometries [36, 37].

2.2. Graphene with point defects

In section 2.1 we assume that graphene has a defect free structure. However, in the real world any material has defects such as impurity atoms and vacancies. These imperfections may appear in the crystal structure naturally, but also might be deliberately introduced [38–42]. Types of disorder in graphene vary widely; however, experimentally point defects are most easily induced [27–29]. We model a defect atom by changing its hopping constant(s). If one of the atoms in the usual basis of graphene with two atoms is modified, we end up with a composite structure such as an alloy with a concentration of 50%. In order to reduce this concentration to reasonable values, we use a 2×2 unit cell as shown in figure 1(b). Thus with this enlargement we obtain a defect concentration of 12.5%. The defects in our system are well separated ($\sim$10 Å) but form a regular lattice. The edge states have an important role in quantum Hall physics and it would be interesting to carry out similar calculations for a finite system such as a graphene nanoribbon. The tight-binding formalism is well suited for such calculations because of the short hopping range of electrons. The termination of graphene at the edges, such as armchair or zigzag, will determine the nature of the edge states. However, such states will be localized to within a few lattice constants, similar to the impurity states considered in this paper. So, the effect of the edge states on magnetotransport is subtle. Whenever the Fermi energy lies in a gap, longitudinal conductivity is zero and Hall conductivity is topologically protected [10]. Thus, as long as there is no scattering between edge states from opposite ends of the ribbon, the Hall conductivity will not change. Significant scattering between edge states is not possible unless the ribbon is only a few lattice constants thick. Thus, our results regarding Hall conductivity in this paper are robust with respect to the boundary conditions, i.e. termination of graphene at the edges.

The natural defects are of course randomly scattered throughout the sample. However, as long as the defect concentration is low, the main effect of defects on transport is through their action as individual scatterers. Thus, in this paper, we model the impure system by considering a regular lattice of point defects as explained above. As long as the point defects create states which are well localized, they can be modeled by enlarging the unit cell [43]. Furthermore, the Hall conductance is a very robust physical quantity, as it can be related to certain topological invariants [10, 20, 44, 45]. We expect that our model closely represents the properties of randomly scattered impurities as long as the conditions above are met.

The enlarged unit cell is shown in figure 1(b). The smaller parallelogram in which the atoms are labeled $a, b, c, \ldots, h$ and index 1 is the enlarged unit cell. The tight-binding procedure is similar to the usual unit cell of graphene; however, since we have eight atoms, our Hamiltonian is now an 8×8 matrix. All the elements of this matrix contain the p_z orbital interactions between the first nearest neighbors and the second order neighbors, if necessary. The magnetic field is introduced to the system via Peierls substitution with the Landau gauge. Different from the previous calculation in section 2.1, the magnetic phase factors are now $4q$ periodic. As a result of this and having eight atoms in the basis, we end up with a $32q \times 32q$ A_{m} matrix. The eigenvalues of the A_{m} matrix give the Hofstadter butterfly spectrum of defective graphene. The detailed description of the tight-binding method applied to defective graphene under magnetic field can be found in [32]. When the Kubo formula is applied to the eigenvalues and eigenvectors of the A_{m} matrix, which is now our magnetic Hamiltonian, we get the Hall conductance as a function of Fermi energy and magnetic field. We define α as $\alpha = p/q = \phi/\phi_0$, where ϕ_0 is the flux quantum and ϕ is the amount of flux per *enlarged* unit cell. We calculate the Hall conduction in the presence of point defects up to second nearest neighbors for p_z orbitals.

3. Results and discussion

By changing the ratio α by means of changing q, one can work in either the low or high magnetic field regimes. For the high magnetic field regime, we see a similar behavior of the Hall conductance to the square lattice case. The value of Hall conductance is given by the Chern numbers, which come as the solutions for the Diophantine [10, 46] equation when the Fermi energy lies in the gaps. For the square lattice the hall conductance σ_{xy} is given as $n \times e^2/h$, with $n = +1, -1, 0$ when $q = 3$ for the Fermi energy is in a gap. The case for the graphene is slightly different from this; for the single value of $q = 3$, the Hall conductance is given by $\sigma_{xy} = n \times e^2/h$ with

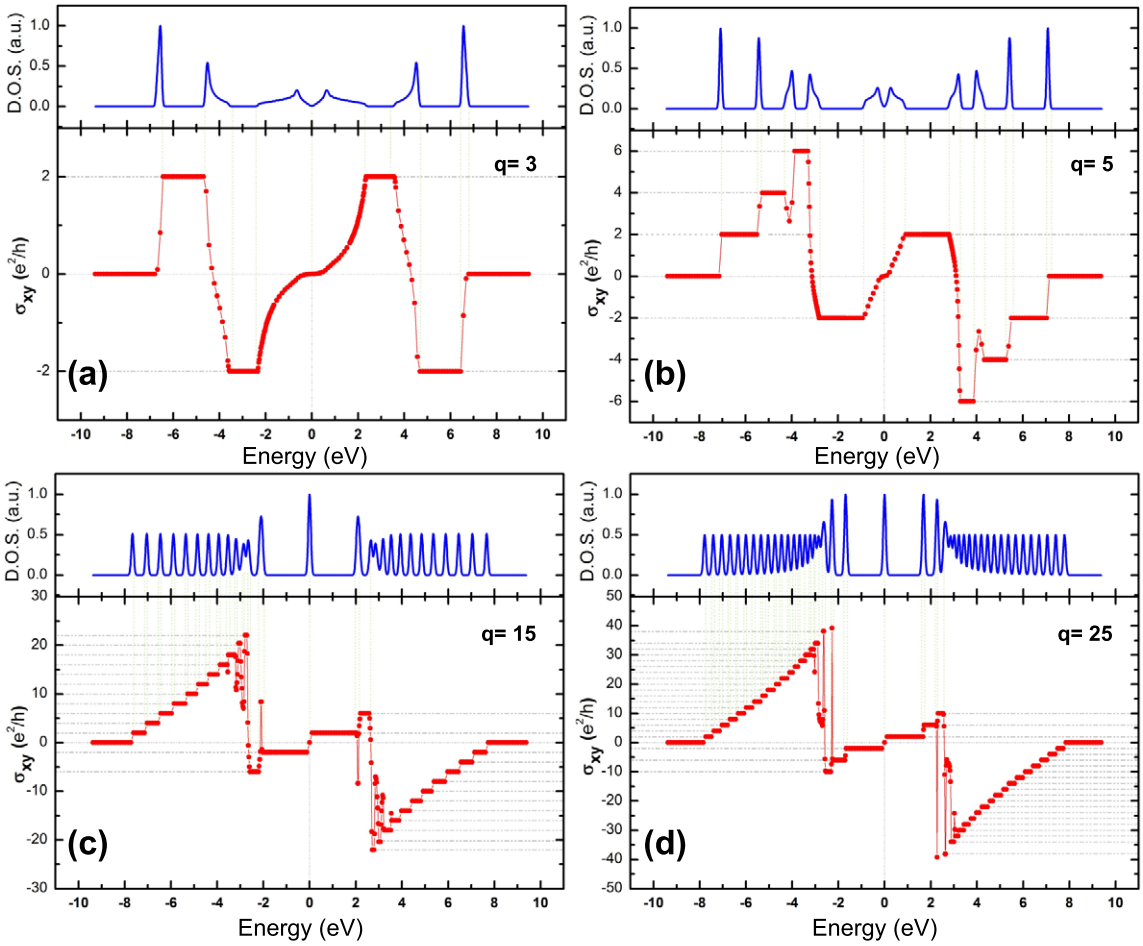

Figure 2. (a) The Hall conductance spectrum for graphene with $q = 3$ and $p = 1$. The plateaus have constant conductances proportional to $n \times e^2/h$, where $n = +2, -2, +2, -2, 0$. (b) The Hall conductance spectrum for graphene with $q = 5$ and $p = 1$. The plateaus have constant conductances proportional to $n \times e^2/h$, where $n = +2, +4, +6, -2, +2, -6, -4, -2, 0$. (c) The Hall anomalous conductance spectrum for graphene with $q = 15$ and $p = 1$. The plateaus around $E_F = 0$ have constant conductances proportional to $n \times e^2/h$, where $n = -6, -2, +2, +6$. The steps have conductance values as a set of even integers. (d) The Hall anomalous conductance spectrum for graphene with $q = 25$ and $p = 1$. The plateaus around $E_F = 0$ have constant conductances proportional to $n \times e^2/h$, where $n = -10, -6, -2, +2, +6, +10$. The insets are the density of states data.

$n = +2, -2, +2, -2, 0$. The Hall conductance in major gaps of the spectrum is displayed in figure 2(a) in units of e^2/h.

Similarly, when we have $q = 5$ given in figure 2(b), we have the conductances as $n = +2, +4, +6, -2, +2, -6, -4, -2, 0$. This behavior of Hall conductance is similar to the results of the square lattice except for the extra factor of 2 originating due to the spin degeneracy in graphene. However, the most interesting case arises when the magnetic field is reduced in magnitude. For both $q = 3$ and 5, we are still working with really high order magnetic field. In the experiments performed in 2005 [17, 18], the anomalous quantum Hall effect was observed for magnetic fields of the order of 10 T.

This strange behavior of conductance is that it is equal to $2(2n + 1)e^2/h$, where n is 0, 1, 2, 3, ... We see that this anomalous quantum Hall regime can be probed even with $q = 15$. The corresponding conductance is displayed in figure 2(c). On setting q to 15 we observe two plateaus around -3 eV $\leq E_F \leq 0$ eV with the conductances given by $-2(2n + 1)e^2/h$, with $n = 0, 1$. A similar structure appears within 0 eV $\leq E_F \leq 3$ eV, with Hall conductances $2(2n + 1)e^2/h$, where $n = 0, 1$. These plateaus are surrounded by scattered-like conductance values, due to the van Hove singularities in the density of states. As we look from the bottom limit of the E_F, we see the step-like increasing conductance, which is the electron-like conductance behavior. Each step increases the conductance by a factor of two in this region, where the gaps are wider than the bands [20]. The same behavior has a mirror image for the Fermi energies on the positive axis as a result of bipartite symmetry of the lattice, since we are just considering the first order interactions. For this case, the observed behavior is the hole-like conductance behavior. A similar spectrum can be seen for $q = 25$ displayed in figure 2(d), where the anomalous quantum Hall conductance plateaus have constant conductances with $-2(2n+1)e^2/h$ and $2(2n + 1)e^2/h$ where $n = 0, 1, 2$. It is also reported that the Hall conductances are given by multiples of Chern numbers when the Fermi energy lies in a gap [20]. In that study, they divide Fermi energy axis into intervals with respect to the magnitude of the hopping constant. They give the value of

the Hall conductance as different functions of Dirac–Landau level indices depending on which interval the Fermi energy lies within ($\times 2$ due to the spin degeneracy). Although they calculate the Hall conductances for the entire energy region, they are able to find the value of the Hall conductance only when the Fermi energy lies in a gap. However, the Kubo formula allows us to calculate the Hall conductance regardless of the position of the Fermi energy. As reported in [20], the Hall conductance displays qualitatively different behavior in the energy range between the van Hove singularities. (See figure 2(d).) The change of electron-like conduction into anomalous integer quantum Hall conduction (anomalous integer quantum Hall conduction into hole-like conduction on the positive Fermi energy axis) occurs in the region of van Hove singularities. In those regions, calculation of Hall conductance requires very fine meshing of k points, as a result of which our conduction values show a scattered structure. However, two main regimes of Hall conduction, integer quantum Hall effect and anomalous integer quantum Hall effect, can still be observed clearly. We achieve the anomalous integer quantum Hall effect for graphene when the magnitude of the magnetic field is reduced; also, we observe 'even' integer quantum Hall effect through higher magnetic fields. When the magnetic field magnitude is reduced by means of increasing the value of q, we see five different behavior regions. Starting from the smallest value of the E_{F}, the first region is the electron-like conduction region, the second one is the scattered conductance region due to the van Hove singularities for the corresponding region of the density of states, then comes the anomalous quantum Hall effect region, with the neighbor of the other van Hove singularities region, and last comes the hole-like conduction region.

We examine the effects of point defects on the Hall conductance for two cases: first with only the nearest neighbor interactions are considered, and second when next nearest hopping is also included. The results for the first nearest neighbors are given as a set of impurity hopping constant strengths in figure 3. The conductance values are distributed symmetrically over right and left hand sides of the entire region of Fermi energy as a result of lattice bipartite symmetry [6]. Since the Hall conduction is calculated for a single value of α, we set it to $\alpha = p/q = 7/3$. We tried to keep q as small as possible because it is a parameter that defines the size of A_{m} matrix ($32q \times 32q$) to be diagonalized. We model several scenarios for the atom labeled '**e**' being different atoms or just a vacancy located at the atomic position of one of the carbon atoms. Part (a) corresponds to the case where the atom '**e**' is an impurity with twice the usual hopping constant. The integer quantum Hall effect with even steps can be observed. Part (c) is the pure case where all the atoms including the atom '**e**' are carbon atoms. One of the differences between parts (a) and (c) is that the widths of the plateaus are narrowed down in part (a) with respect to the pure case. Also, this impurity atom modifies the conduction at the bottom and top regions of the Fermi energy scale. This larger hopping constant impurity brings out new conduction plateaus at around $E_{\mathrm{f}} \simeq -10$ eV and $E_{\mathrm{f}} \simeq 10$ eV with Hall conductance of $-2e^2/h$ and $2e^2/h$ separated from the ones in the pure case with plateaus of zero Hall conductance, respectively. A similar behavior still survives when the hopping constant of atom '**e**' is reduced to $\frac{3}{2}H_{\mathrm{pp}\pi}$, given in part (b). This additional Hall plateaus occur due to an increase in the interaction of the impurity atom with the neighboring atoms. The states due to this kind of impurity appear to be delocalized and they contribute to Hall conduction.

The rest of the parts in figure 3 constitute a second set where the atom '**e**' is again an impurity, but this time its hopping constant is reduced to several fractions of the rest of the atoms. Part (d) represents the case of an impurity with $H^{\mathrm{E}}_{\mathrm{pp}\pi} = \frac{3}{4}H_{\mathrm{pp}\pi}$. We see that there are still plateaus with zero Hall conduction for -5 eV $\leq E_{\mathrm{f}} \leq -2.5$ eV (and 2.5 eV $\leq E_{\mathrm{f}} \leq 5$ eV), but this time they are not followed by $\pm 2e^2/h$ conduction plateaus. In addition, the plateaus with conduction values of $-6e^2/h$ and $6e^2/h$ in the regions -7.5 eV $\leq E_{\mathrm{f}} \leq -5$ eV and 5 eV $\leq E_{\mathrm{f}} \leq 7.5$ eV are reduced to $-4e^2/h$ and $4e^2/h$. Moreover, the constant conduction of $-2e^2/h$ and $2e^2/h$ lying in the regions -6.4 eV $\leq E_{\mathrm{f}} \leq -4.6$ eV and 4.6 eV $\leq E_{\mathrm{f}} \leq 6.4$ eV for the pure case now split with a plateau of zero conductance. This splitting increases as we keep reducing the hopping parameter of atom '**e**' seen in parts (e) and (f), and it has its maximum width in part (g), where atom '**e**' is the vacancy. When we look at the general trend of Hall conduction in parts (e) and (f), we see that the conduction is suppressed with respect to the pure case. As we end up with the vacancy case shown in the last part, there remain only the plateaus with $-2e^2/h, 2e^2/h$ and zero conductance. We can state that, by reducing the hopping constant of atom '**e**', we are interrupting the conduction mechanism. The states due to this kind of impurity appear to be highly localized on the defect atoms in the entire magnetic unit cell, as a result of which they have no contribution to the conductance; rather, they suppress the Hall conduction mechanism. As the impurity states are highly localized, our results should not be modified by the random distribution of defects.

The Hall conductance in the presence of the second order interactions is depicted in figure 4 as a complementary set to figure 3. Due to the breaking of the bipartite symmetry of the lattice by introducing the second order interactions, the conductance values are no longer symmetrically distributed over the whole region of Fermi energy. Similar to the previous calculation, the value of α is equal to 7/3. We observe that the Hall conductance values are robust with respect to the second order interactions in graphene. However the widths of the plateaus are changed as the widths of the gaps and bands are modified. The larger hopping constant impurity results in new nonzero Hall conduction values, by modifying conduction values around the bottom and the top regions of the Fermi energy. Similar to the first order calculations, the impurity atoms with smaller hopping constants do not contribute to Hall conduction. Their presence suppresses the conduction, and as we keep reducing the hopping constants we only get conduction plateaus with $-2e^2/h, 2e^2/h$ and zero conductance.

In figure 5, portions of Hofstadter butterflies for imperfect graphene are displayed with Hall conductances indicated in the major gaps. In figure 5(a), only the first order interactions

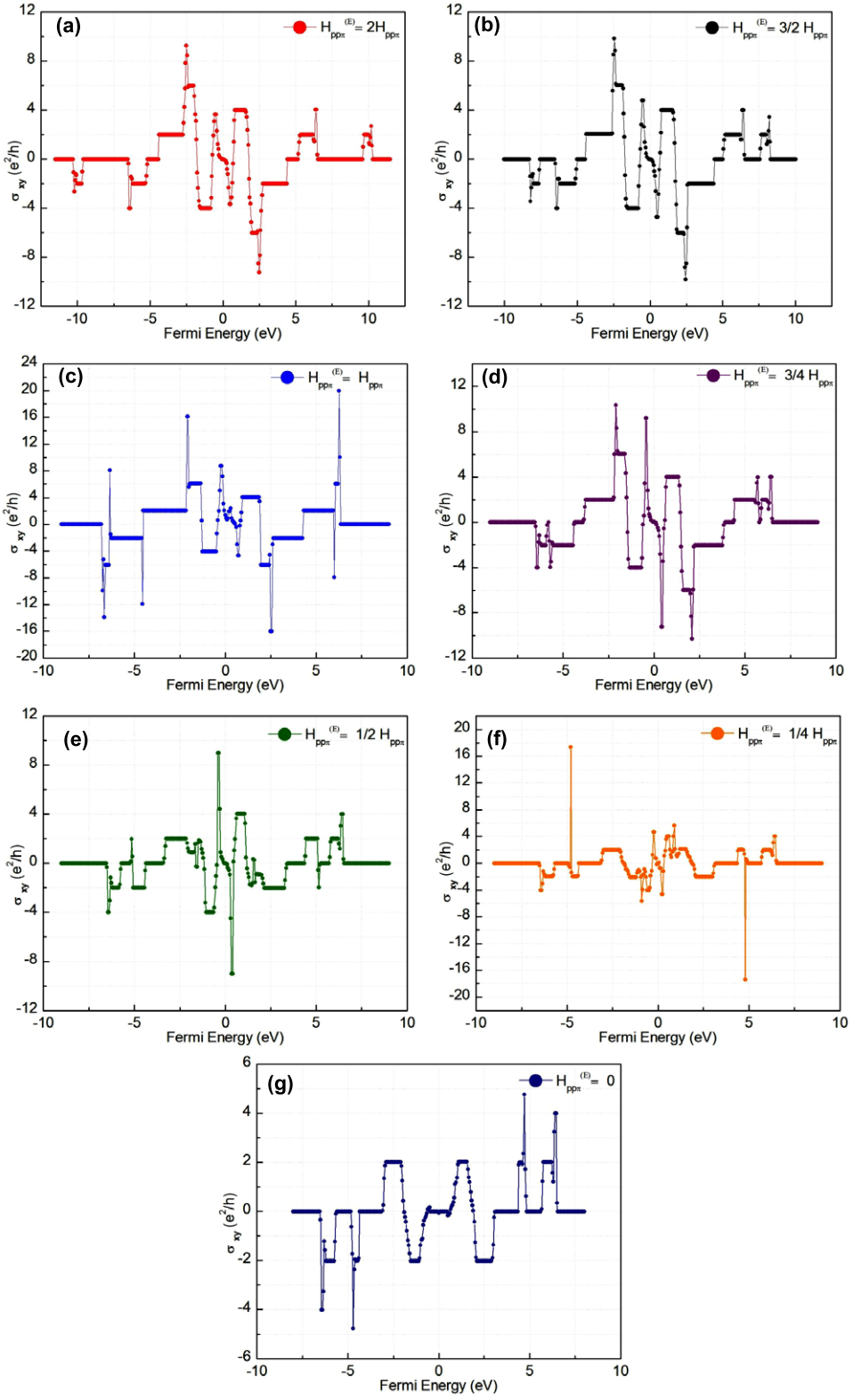

Figure 3. Integer quantum Hall conductance for graphene with point defects; only the first order interactions are considered. For all of the calculations $\alpha = p/q = 7/3$; (a) $H^{\mathrm{E}}_{\mathrm{pp}\pi} = 2H_{\mathrm{pp}\pi}$, (b) $H^{\mathrm{E}}_{\mathrm{pp}\pi} = \frac{3}{2}H_{\mathrm{pp}\pi}$, (c) $H^{\mathrm{E}}_{\mathrm{pp}\pi} = H_{\mathrm{pp}\pi}$, (d) $H^{\mathrm{E}}_{\mathrm{pp}\pi} = \frac{3}{4}H_{\mathrm{pp}\pi}$, (e) $H^{\mathrm{E}}_{\mathrm{pp}\pi} = \frac{1}{2}H_{\mathrm{pp}\pi}$, (f) $H^{\mathrm{E}}_{\mathrm{pp}\pi} = \frac{1}{4}H_{\mathrm{pp}\pi}$, and (g) $H^{\mathrm{E}}_{\mathrm{pp}\pi} = 0$.

are assumed to exist. The x-axis has the values for $\alpha = p/q = \phi/\phi_0$, where ϕ is the amount of magnetic flux per *enlarged* unit cell. The atom '**e**' has a hopping strength one fourth of that of the other atoms. The corresponding Hall conduction is given in figure 3(f) for $\alpha = 7/3$. The gaps with Hall conduction $\pm 6e^2/h$, $\pm 4e^2/h$ are observed in

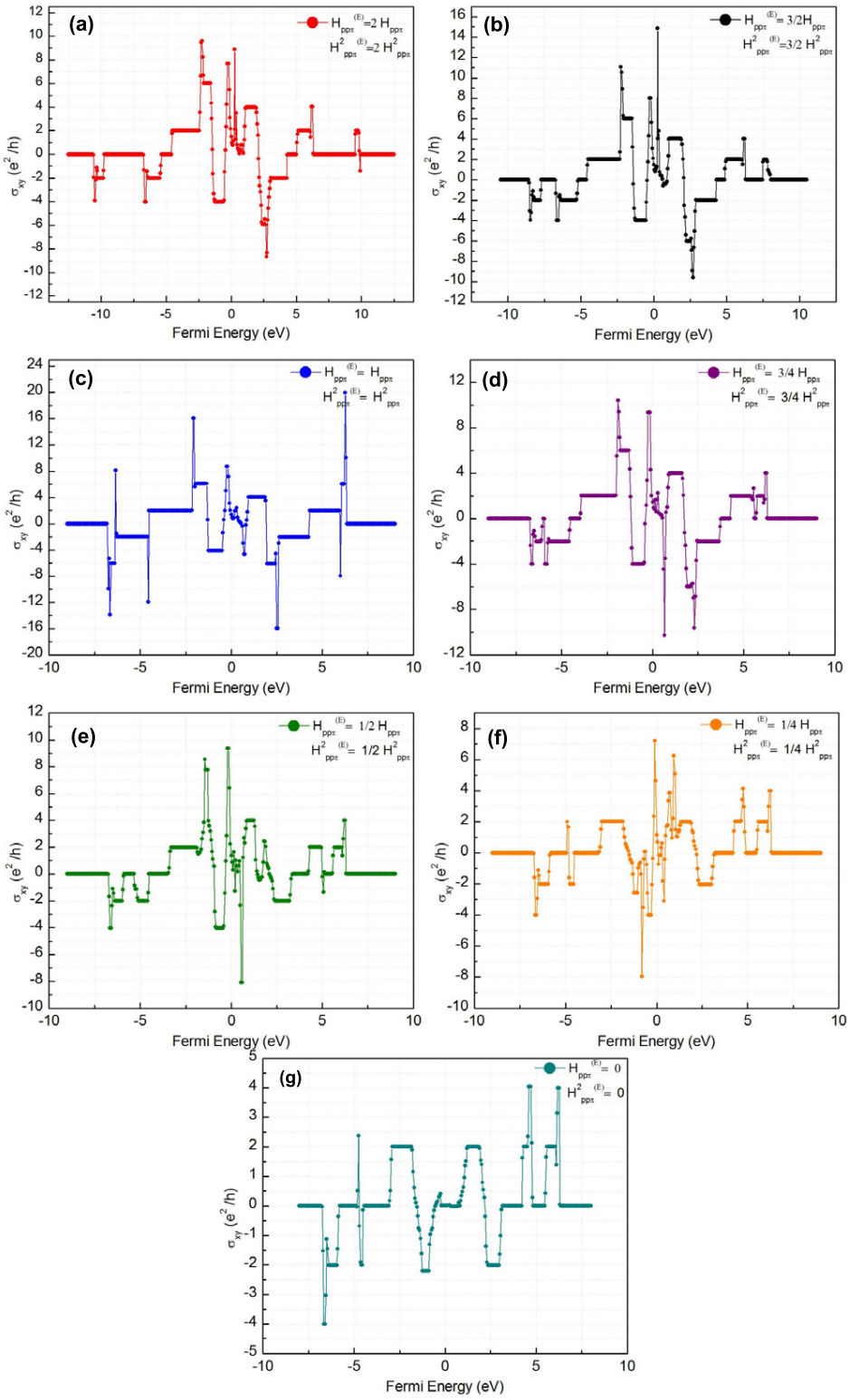

Figure 4. Integer quantum Hall conductance for graphene with point defects; both the first and the second order interactions are considered. For all of the calculations $\alpha = p/q = 7/3$; (a) $H^{\mathrm{E}}_{\mathrm{pp}\pi} = 2H_{\mathrm{pp}\pi}$ and $H^{2(E)}_{\mathrm{pp}\pi} = 2H^2_{\mathrm{pp}\pi}$, (b) $H^{\mathrm{E}}_{\mathrm{pp}\pi} = \frac{3}{2}H_{\mathrm{pp}\pi}$ and $H^{2(E)}_{\mathrm{pp}\pi} = \frac{3}{2}H^2_{\mathrm{pp}\pi}$, (c) $H^{\mathrm{E}}_{\mathrm{pp}\pi} = H_{\mathrm{pp}\pi}$ and $H^{2(E)}_{\mathrm{pp}\pi} = H^2_{\mathrm{pp}\pi}$, (d) $H^{\mathrm{E}}_{\mathrm{pp}\pi} = \frac{3}{4}H_{\mathrm{pp}\pi}$ and $H^{2(E)}_{\mathrm{pp}\pi} = \frac{3}{4}H^2_{\mathrm{pp}\pi}$, (e) $H^{\mathrm{E}}_{\mathrm{pp}\pi} = \frac{1}{2}H_{\mathrm{pp}\pi}$ and $H^{2(E)}_{\mathrm{pp}\pi} = \frac{1}{2}H^2_{\mathrm{pp}\pi}$, (f) $H^{\mathrm{E}}_{\mathrm{pp}\pi} = \frac{1}{4}H_{\mathrm{pp}\pi}$ and $H^{2(E)}_{\mathrm{pp}\pi} = \frac{1}{4}H^2_{\mathrm{pp}\pi}$, and (g) $H^{\mathrm{E}}_{\mathrm{pp}\pi} = 0$ and $H^{2(E)}_{\mathrm{pp}\pi} = 0$.

the neighborhood of $E_f = 0$ eV, which is not observed in figure 3(f) as only a single α value is considered. Figure 5(b) is the case when the second order interactions are involved. The breaking of bipartite symmetry results in shifting of gaps and bands with respect to the $E = 0$ eV line. This specific case is the case which has the impurity atoms with $H^{\mathrm{E}}_{\mathrm{pp}\pi} =$

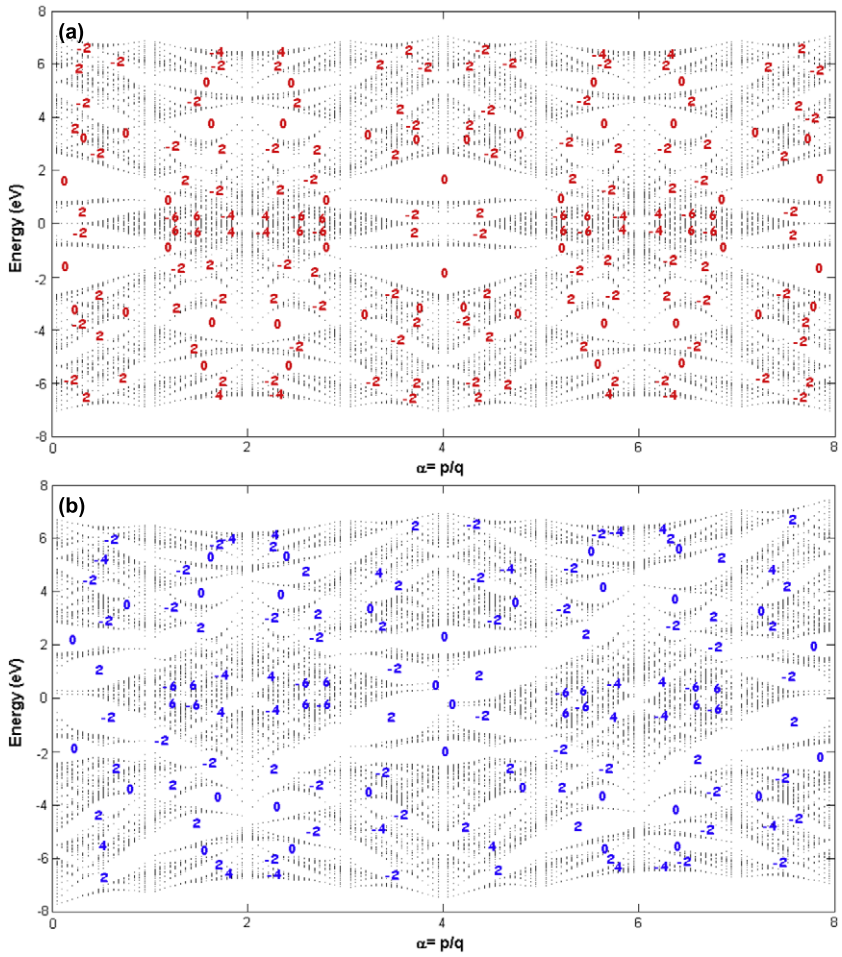

Figure 5. Portion of Hofstadter butterflies for graphene with point defects. The Hall conduction values of main gaps are marked on the graphs. (a) First order interactions; the atom labeled '**e**' has $H^{\mathrm{E}}_{\mathrm{pp}\pi} = \frac{1}{4}H_{\mathrm{pp}\pi}$. (b) Both the first and the second order interactions are involved; the atom labeled '**e**' has $H^{\mathrm{E}}_{\mathrm{pp}\pi} = \frac{1}{2}H_{\mathrm{pp}\pi}$ and $H^{2(E)}_{\mathrm{pp}\pi} = \frac{1}{2}H^{2}_{\mathrm{pp}\pi}$.

$\frac{1}{2}H_{\mathrm{pp}\pi}$ and $H^{2(E)}_{\mathrm{pp}\pi} = \frac{1}{2}H^{2}_{\mathrm{pp}\pi}$. The same $\pm 6e^2/h$, $\pm 4e^2/h$ valued conduction gaps are still there. Regardless of the effect of second order interactions, the widths of these gaps are larger in comparison with figure 5(a). Hence, our claim that suppression of the Hall conductance—by means of narrowing of the plateaus—increases with the reduction of the hopping constant of the impurity atom is once again verified.

The effect of impurity atoms on the energy can be visualized in figure 6. We take $\alpha = p/q = 80/31 \simeq 2.58$, and consider both the first and the second order interactions. We can keep track of the conduction values for the gaps roughly from figure 4 for the vertical dotted lines. Since the Hall conductance is a topological invariant within a gap, its value does not change unless the bands cross. Thus the conductance value within the major gaps can be easily discerned from the calculation at a single t'/t value. The impurities with smaller hopping constants modify the Hofstadter butterfly mostly around the $E = 0$ eV line. As the impurity hopping strengths are increased to $H_{\mathrm{pp}\pi} = t = t'$, we see new gap and band formation around that region. In addition, the width of the spectrum is constant for $t'/t \leq 1$. However, the spectrum displays unusual behavior beyond this point. For the impurities with greater hopping constants, some bands are separated from the rest of the energy spectrum around the minimum and the maximum. The original spectrum mostly remains intact. As we increase the hopping strength to higher values, we see that these bands gain their own self-similar structure separated by zero conductance gaps from the original spectrum. This separation happens roughly around $t'/t = 1.2$. Beyond $t'/t \geq 1.5$, the bulk of the spectrum remains unchanged while two impurity bands further separate, increasing the zero conductance gaps. The Hall conduction plateaus with $\sigma_{xy} = \pm 2e^2/h$ presented in figure 4 are located within these bands. As a result, we observe that the higher hopping constant impurities produce their own self-similar band by modifying the energy spectrum around the top and the bottom values of the energy. A shortcoming of our model is the periodic arrangement of the defect atoms. This periodic arrangement results in well defined $\sigma_{xy} = \pm 2e^2/h$ conduction plateaus within these separated bands and their overall self-similar behavior. However, in a real sample the impurities would be distributed over the system randomly. Although this randomness would disturb the self-similar structure of these bands, it is not expected to significantly

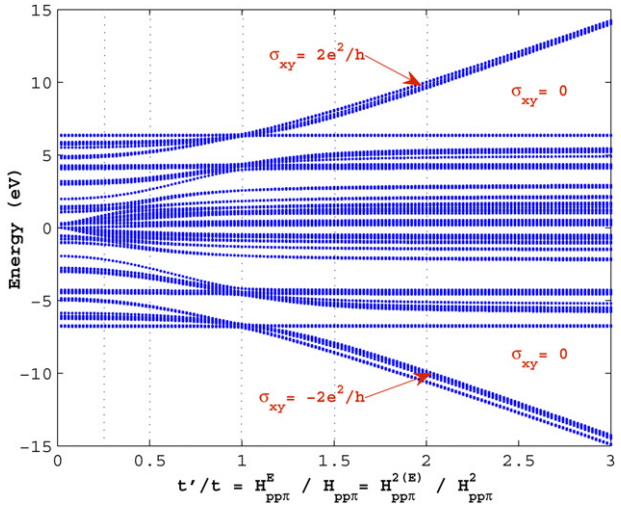

Figure 6. The change in the band structure of impure graphene as a function of impurity hopping strength. $p = 80$ and $q = 31$; both the first and the second neighbor interactions are considered. The conduction values along the vertical dotted lines can be inspected from figure 4. The impurity bands leave the bulk of the spectrum and create their own self-similar structure with the critical value of the impurity hopping strength $t'/t \geq 1.2$. The higher hopping constant impurities are responsible for the gaps with nonzero Hall conductance values beyond this point.

modify their energies. As beyond $t'/t \geq 1.5$ the impurity bands are separated from the bulk of the spectrum by large gaps, their behavior should be mostly independent. These independent bands would still survive under randomness; however, one would not expect Hall conduction plateaus within these bands, or any well defined self-similarity with regard to defect states.

The anomalous integer quantum Hall effect can be observed for impure graphene, too. However, modeling graphene with point defects of reasonable concentration requires high computational cost. We model defects with 12.5% concentration, which needs a $32q \times 32q$ matrix diagonalization. In order to see the anomalous quantum Hall effect which happens at large $q \geq 15$ (figure 2), we should have larger values for q, which automatically increases the computation time enormously with a sufficient amount of k-point meshing.

4. Conclusions

In conclusion, we applied the Kubo conductance formula to graphene in order to investigate the magnetoconductance properties. For pure graphene our results clearly display the usual and the anomalous quantum Hall effects, even though our magnetic fields are much higher than the usual experimental values. This physical limitation for the magnitude of the magnetic field can be overcome by some other indirect methods. For example, it was reported [47] that the shear strain applied to graphene results in a pseudomagnetic field. There is an extra phase factor arising due to the shear strain, which makes the problem identical to the magnetic field application from the point of view of the tight-binding method. Our calculations show that, even when the magnetic field is large enough to preclude a continuum Dirac equation description of electronic conduction, anomalous and normal integer quantum Hall effects are present for graphene. The anomalous Hall effect is always sandwiched between the usual Hall effect regions with van Hove singularities marking the boundaries between them.

The point defects which are natural ingredients of graphene have interesting effects on the Hall conduction. The defect atoms with smaller hopping constants do not make major contributions to Hall conductance. The states originating from these weakly coupled impurity atoms are highly localized on the defect atoms. This localization is at its maximum for the vacancy case. On the other hand, by increasing the hopping constant of the impurity atoms we increase the interaction of these sites with the neighboring ones. Hence, the states corresponding to strongly coupled impurities are delocalized. Such delocalized states form separate bands at the extrema of the spectrum, creating large, zero Hall conductance gaps. The bulk of the spectrum and corresponding magnetoconductance properties are not modified by these impurity states.

Acknowledgment

MÖO acknowledges partial support from TÜBİTAK, the Scientific and Technological Research Council of Turkey (grant no TBAG 109T267).

References

[1] Hofstadter D R 1976 *Phys. Rev.* B **14** 2239
[2] Albrecht C, Smet J H, von Klitzing K, Weiss D, Umansky V and Schweizer H 2001 *Phys. Rev. Lett.* **86** 147
[3] Analytis J G, Blundell S J and Ardavan A 2004 *Am. J. Phys.* **72** 613
[4] Hasegewa Y, Hatsugai Y, Kohmoto M and Montambaux G 1990 *Phys. Rev.* B **41** 9174
[5] Hasegewa Y and Kohmoto M 2006 *Phys. Rev.* B **74** 155415
[6] Rammal R 1985 *J. Physique* **46** 1345
[7] Nemec N and Cuniberti G 2006 *Phys. Rev.* B **74** 165411
[8] Gumbs G and Fekete P 1997 *Phys. Rev.* B **56** 3787
[9] İslamoğlu S, Oktel M Ö and Gülseren O 2012 *J. Phys.: Condens. Matter* **24** 345501
[10] Thouless D J, Kohmoto M, Nightingale M P and den Nijs M 1982 *Phys. Rev. Lett.* **49** 405
[11] Kohmoto M 1985 *Ann. Phys., NY* **160** 343
[12] Streda P 1982 *J. Phys. C: Solid State Phys.* **15** L717
[13] Novoselov K S, Geim A K, Morozov S V, Jiang D, Zhang Y, Dubonos S V, Grigorieva I V and Firsov A A 2004 *Science* **306** 666
[14] Novoselov K S, Jiang D, Schedin F, Booth T J, Khotkevic V V, Morozov S V and Geim A K 2005 *Proc. Natl Acad. Sci. USA* **102** 10451
[15] Zheng Y and Ando T 2002 *Phys. Rev.* B **65** 245420
[16] Gusynin V P and Sharapov S G 2005 *Phys. Rev. Lett.* **95** 146801
[17] Novoselov K S, Geim A K, Morozov S V, Jiang D, Katsnelson M I, Grigorieva I V, Dubonos S V and Firsov A A 2005 *Nature* **438** 197
[18] Zhang Y, Tan Y-W, Stormer H L and Kim P 2005 *Nature* **438** 201

[19] Peres N M R, Guinea F and Castro Neto A H 2006 *Phys. Rev.* B **73** 125411
[20] Hatsugai Y, Fukui T and Aoki H 2006 *Phys. Rev.* B **74** 205414
[21] Bernevig B A, Hughes T L, Zhang S C, Chen H D and Wu C 2006 *Int. J. Mod. Phys.* B **20** 3257
[22] Sato M, Tobe D and Kohmoto M 2008 *Phys. Rev.* B **78** 235322
[23] Esquinazi P, Spemann D, Höhne R, Setzer A, Han K-H and Butz T 2003 *Phys. Rev. Lett.* **91** 227201
[24] Hashimoto A, Suenaga K, Gloter A, Urita K and Iijima S 2004 *Nature* **430** 870
[25] Lehtinen P O, Foster A S, Ma Y, Krasheninnikov A V and Nieminen R M 2004 *Phys. Rev. Lett.* **93** 187202
[26] Yazyev O V and Helm L 2007 *Phys. Rev.* B **75** 125408
[27] Teweldebrhan D and Balandin A A 2009 *Appl. Phys. Lett.* **94** 013101
[28] Liu G, Teweldebrhan D and Balandin A A 2011 *IEEE Trans. Nanotechnol.* **10** 865
[29] Chen S, Wu Q, Mishra C, Kang J, Zhang H, Cho K, Cai W, Balandin A A and Ruoff S R 2012 *Nature Mater.* **11** 203
[30] Koshino M and Ando T 2007 *Phys. Rev.* B **75** 033412
[31] Sheng D N, Sheng L and Weng Z Y 2006 *Phys. Rev.* B **73** 233406
[32] İslamoğlu S, Oktel M Ö and Gülseren O 2012 *Phys. Rev.* B **85** 235414
[33] Charlier J-C, Lambin Ph and Ebbesen T W 1996 *Phys. Rev.* B **54** 8377
[34] Peierls R 1933 *Z. Phys.* **80** 763
[35] Harper P G 1955 *Proc. Phys. Soc.* A **68** 874
[36] Li J, Wang Y-F and Gong C-D 2011 *J. Phys.: Condens. Matter* **23** 156002
[37] Wang Y-F and Gong C-D 2010 *Phys. Rev.* B **82** 113304
[38] Schedin F, Geim A K, Morozov S V, Hill E W, Blake P, Katsnelson M I and Novoselov K S 2007 *Nature Mater.* **6** 652
[39] Chen J-H, Jang C, Adam S, Fuhrer M S, Williams E D and Ishigami M 2008 *Nature Phys.* **4** 377
[40] Wehling T O, Balatsky A V, Katsnelson M I, Lichtenstein A I, Scharnberg K and Wiesendanger R 2007 *Phys. Rev.* B **75** 125425
[41] Tan Y-W, Zhang Y, Bolotin K, Zhao Y, Adam S, Hwang E H, Das Sarma S, Stormer H L and Kim P 2007 *Phys. Rev. Lett.* **99** 246803
[42] Zhang H, Lazo C, Blügel S, Heinze S and Mokrousov Y 2012 *Phys. Rev. Lett.* **108** 056802
[43] Van de Walle C G and Neugebauer J 2004 *J. Appl. Phys.* **95** 3851
[44] Laughlin R B 1981 *Phys. Rev.* B **23** 5632
[45] Laughlin R B 1983 *Phys. Rev. Lett.* **50** 1395
[46] Kohmoto M 1989 *Phys. Rev.* B **39** 11943
[47] Levy N, Burke S A, Meaker K L, Panlasigui M, Zettl A, Guinea F, Castro Neto A H and Crommie M F 2010 *Science* **329** 544